



Bovine respiratory syncytial (RS) virus : experimental infection in African pygmy goats  
by John Andrew Blixt

A thesis submitted in partial fulfillment of the requirements for the degree of MASTER OF SCIENCE  
in Veterinary Science  
Montana State University  
© Copyright by John Andrew Blixt (1981)

**Abstract:**

African pygmy goats were experimentally infected with a bovine respiratory syncytial virus. There were no signs of clinical disease in infected goats.

Histological and ultrastructural studies were performed to examine the effects of respiratory syncytial virus on the bronchi, bronchioles and alveolar epithelium. Histologically, a bronchial plug consisting of cell debris, macrophages and lymphocytes was observed in one goat. Changes in bronchioles consisted of a peribronchiolar infiltration with monocytes. The alveolar septa in two goats were thickened due to fibrosis, infiltrating monocytes and polymorphonuclear leukocytes in the alveolar connective tissue. Ultrastructurally, respiratory syncytial virus maturation occurred at the plasma membrane. Virions were observed budding from the plasma membrane of ciliated cells and nonciliated nonsecretory cells in bronchioles, and from the plasma membrane of type I and type II alveolar pneumonocytes.

This study suggested the African pygmy goat may be a suitable animal model for bovine respiratory disease.

STATEMENT OF PERMISSION TO COPY

In presenting this thesis in partial fulfillment of the requirements for an advanced degree at Montana State University, I agree that the Library shall make it freely available for inspection. I further agree that permission for extensive copying of this thesis for scholarly purposes may be granted by my major professor, or, in his absence, by the Director of Libraries. It is understood that any copying or publication of this thesis for financial gain shall not be allowed without my written permission.

Signature

*John A. Blyth*

Date

*Jan. 26, 1981*

BOVINE RESPIRATORY SYNCYTIAL (RS) VIRUS:  
EXPERIMENTAL INFECTION IN AFRICAN PYGMY GOATS

by

JOHN ANDREW BLIXT

A thesis submitted in partial fulfillment  
of the requirements for the degree


of


MASTER OF SCIENCE


in

Veterinary Science

Approved:

  
Chairman, Graduate Committee

  
Head, Major Department

  
Graduate Dean

MONTANA STATE UNIVERSITY  
Bozeman, Montana

January, 1981

## ACKNOWLEDGMENTS

The author would like to express sincere appreciation to Dr. Herb Smith and Dr. Glen Epling for their understanding, guidance and support throughout this study.

He would like to thank his graduate committee for their contributions and advice. Thanks also go to Dr. Tom Carroll for teaching basic techniques in electron microscopy and to Don Fritts for teaching his methods in biomedical photography. A special thanks goes to Sandra Phillips and Donna Gollehon for their assistance in cell culture methods and to Susie Patterson, Jonne Shearman and Mary Reilly for the preparation of histological slides and to Betty Freeland for typing the manuscript.

## TABLE OF CONTENTS

	Page
VITA . . . . .	ii
ACKNOWLEDGMENTS . . . . .	iii
LIST OF FIGURES . . . . .	vi
ABSTRACT . . . . .	xi
CHAPTER	
1 INTRODUCTION . . . . .	1
2 LITERATURE REVIEW . . . . .	2
Bronchi and Bronchioles . . . . .	2
Alveolar Epithelium . . . . .	8
Alveolar Damage . . . . .	14
Respiratory Syncytial Virus . . . . .	16
Ultrastructure of Respiratory Syncytial Virus . . . . .	18
Negatively Stained Preparations . . . . .	18
Ultrathin Section . . . . .	21
Pathological Changes . . . . .	23
3 MATERIALS AND METHODS . . . . .	27
Cell Culture and Culture Media . . . . .	27
Stock Virus . . . . .	27
Control Inoculum . . . . .	28
Virus Titration . . . . .	28
Pygmy Goats . . . . .	29
Fixation . . . . .	30
Light Microscopy . . . . .	30
Electron Microscopy . . . . .	31
Transmission Electron Microscopy (TEM) . . . . .	31
Scanning Electron Microscopy (SEM) . . . . .	32
Electron Microscopy of Particle Suspensions . . . . .	32
Electron Microscopy of RSV Infected Cell Culture . . . . .	33
4 RESULTS . . . . .	35
Clinical Signs . . . . .	35

CHAPTER	Page
Negatively Stained RS Virions . . . . .	35
Bovine Turbinate Cell Culture Infected with RSV . . .	36
Normal Goat Lung . . . . .	36
RSV Goat Lung . . . . .	39
Control Goat Lung . . . . .	42
Comparative Distribution of Microvilli . . . . .	44
5 DISCUSSION . . . . .	110
6 SUMMARY . . . . .	116
LITERATURE CITED . . . . .	117

## LIST OF FIGURES

Figure	Page
1. Negatively stained spherical and filamentous RS virions . . . . .	45
2. Negatively stained spherical RS virions showing club-shaped surface projections . . . . .	47
3. Negatively stained virion displaying a rosette shape . . . . .	48
4. Negatively stained RS pleomorphic virion . . . . .	49
5. Negatively stained pleomorphic virion . . . . .	50
6. RSV maturation at the plasma membrane in cell culture . . . . .	51
7. RSV budding from the plasma membrane in cell culture . . . . .	52
8. LM. Normal lung. Terminal bronchiole (Tb) and alveoli (A) . . . . .	53
9. LM. Normal lung. Respiratory bronchiole (Rb), alveolar duct (ad) and alveolar sac (S) . . . . .	54
10. SEM. Normal lung. Respiratory bronchiole (Rb), alveolar duct (Ad), alveoli (A) and pore of Kohn (P) . . . . .	55
11. SEM. Normal lung. Pore of Kohn (P), type I pneumocyte (I) and type II pneumocyte (II) . . . . .	56
12. SEM. Normal lung. Junction between a type I and type II pneumocyte . . . . .	57
13. SEM. Normal lung. Capillaries in an alveolar wall . . . . .	58
14. SEM. Normal lung. Bronchiole X4,500. Clara cell (Cl), ciliated cell (Ci) . . . . .	59
15. SEM. Normal lung. Clara cell (Cl) in a respiratory bronchiole . . . . .	60

## LIST OF FIGURES (continued)

Figure	Page
16. TEM. Normal lung. Type I alveolar pneumonocyte (I) . . . . .	61
17. TEM. Normal lung. Type I cell with caveolae. . . . .	62
18. TEM. Normal lung. Type I cell over a capillary . . . . .	63
19. TEM. Normal lung. Type I (I) and type II (II) pneumonocytes . . . . .	64
20. TEM. Normal lung. Tight junction connecting a type I and type II pneumonocyte . . . . .	65
21. TEM. Normal lung. A Clara cell (Cl) and nonciliated cell located in a bronchiole. . . . .	66
22. TEM. Normal lung. Merocrine secretion in a Clara cell. . . . .	67
23. TEM. Normal lung. Ciliated cell in a terminal bronchiole with microvilli in longitudinal section . . . . .	68
24. TEM. Normal lung. Ciliated cell with microvilli in cross-section . . . . .	69
25. TEM. Normal lung. High magnification of a cilium dis- playing typical 9+2 configuration . . . . .	70
26. LM. RSV lung showing thickened alveolar septa . . . . .	71
27. LM. RSV lung. Terminal bronchiole displays cellular infiltrate . . . . .	72
28. LM. RSV lung. Higher magnification of infiltrating monocytes and PMNs in fig. 27 . . . . .	73
29. LM. RSV lung. Necrotic epithelium in large bronchus. . . . .	74
30. LM. RSV lung. Edema in lamina propria (arrows) in a large bronchus. . . . .	75
31. LM. RSV lung. Bronchial plug in lumen of a large bronchus . . . . .	76



## LIST OF FIGURES (continued)

Figure	Page
32. SEM. RSV lung. Alveolar wall with type I pneumonocytes . . . . .	77
33. SEM. RSV lung. Type I pneumonocytes display a microvillous hyperplasia or budding virions . . . . .	78
34. SEM. RSV lung. Type I pneumonocytes with increased surface projections and a recess type II (II) cell . . . . .	79
35. SEM. RSV lung. Alveolar wall with many surface projections. . . . .	80
36. SEM. RSV lung. Type II pneumonocyte with secretory blebs . . . . .	81
37. SEM. RSV lung. Type II cell with secretory pit containing surfactant . . . . .	82
38. SEM. RSV lung. Goblet cell surrounded by ciliated cells in a large bronchiole . . . . .	83
39. TEM. RSV lung. Surface projections on type I pneumonocytes . . . . .	84
40. TEM. RSV lung. Type I cell with possible cytoplasmic inclusion body (Cb) located in a paranuclear position . . . . .	85
41. TEM. RSV lung. Filamentous RS virion budding from a type I pneumonocyte . . . . .	86
42. TEM. RSV lung. RS virus budding from plasma membrane of a type I cell . . . . .	86
43. TEM. RSV lung. Spherical and filamentous virions budding from a type I cell . . . . .	87
44. TEM. RSV lung. Type II pneumonocyte with budding RS virions . . . . .	88
45. TEM. RSV lung. Higher magnification of budding virions in Fig. 44 . . . . .	89

## LIST OF FIGURES (continued)

Figure	Page
46. TEM. RSV lung. Numerous spherical virions budding from type II cell . . . . .	90
47. TEM. RSV lung. Higher magnification of type II cell surface with virions in Fig. 46 . . . . .	91
48. TEM. RSV lung. Type II cell with filamentous virions . .	92
49. TEM. RSV lung. Large bronchiole nonciliated cell with filamentous and spherical RS virions . . . . .	93
50. TEM. RSV lung. High magnification of spherical virions budding from a nonciliated cell. . . . .	94
51. TEM. RSV lung. Filamentous virions budding from a ciliated cell in a terminal bronchiole . . . . .	95
52. LM. Control lung. Normal terminal bronchiole and alveoli. . . . .	97
53. SEM. Control lung. Type I and type II pneumonocytes. . .	98
54. SEM. Control lung. Type II cell with secretory blebs and a secretory pit. . . . .	99
55. SEM. Control lung. Secretory droplet protruding from a type II cell . . . . .	100
56. SEM. Control lung. Junction separating a respiratory bronchiole (Rb) and an alveolus (A) . . . . .	101
57. SEM. Control lung. Clara cells (Cl) with secretory blebs in a respiratory bronchiole . . . . .	102
58. SEM. Control lung. Goblet cell (Gc) and nonciliated cell (Nc) in a large bronchiole . . . . .	103
59. TEM. Control lung. Clara cell displaying merocrine type secretion . . . . .	104

LIST OF FIGURES (continued)

Figure	Page
60. TEM. Control lung. Clara cell with similar contents in lumen of a bronchiole . . . . .	105
61. TEM. Control lung. Brush cell (Bc) located in a large bronchiole . . . . .	106
62. SEM. Normal lung. Type I pneumonocyte with sparse microvilli . . . . .	107
63. SEM. Control lung. Type I cell covered sparsely with microvilli . . . . .	108
64. SEM. RSV lung. Type I cell with numerous surface projections . . . . .	109

## ABSTRACT

African pygmy goats were experimentally infected with a bovine respiratory syncytial virus. There were no signs of clinical disease in infected goats.

Histological and ultrastructural studies were performed to examine the effects of respiratory syncytial virus on the bronchi, bronchioles and alveolar epithelium. Histologically, a bronchial plug consisting of cell debris, macrophages and lymphocytes was observed in one goat. Changes in bronchioles consisted of a peribronchiolar infiltration with monocytes. The alveolar septa in two goats were thickened due to fibrosis, infiltrating monocytes and polymorphonuclear leukocytes in the alveolar connective tissue. Ultrastructurally, respiratory syncytial virus maturation occurred at the plasma membrane. Virions were observed budding from the plasma membrane of ciliated cells and nonciliated nonsecretory cells in bronchioles, and from the plasma membrane of type I and type II alveolar pneumonocytes.

This study suggested the African pygmy goat may be a suitable animal model for bovine respiratory disease.

## CHAPTER 1

### INTRODUCTION

The respiratory syncytial virus (RSV) is an important respiratory tract pathogen in human infants under the age of 1 year and is common in infections in the adult human population. Serological surveys demonstrated that neutralizing antibodies for the virus were present in 90% of the population by 15 years of age (13, 25-27, 54).

The bovine RSV is worldwide in distribution and is an important etiological agent in the bovine respiratory disease complex (BRDC) (59, 84, 90, 92). Since the BRDC is of multiple etiology, it is extremely difficult to evaluate the role of RSV. Experimental RSV infections are rarely fatal in calves, but can decrease the host's resistance to allow other pathogens to complicate the complex (23).

In order to study the pathogenesis of RSV a good animal model is needed. Cebus monkeys have been partially evaluated and were shown to develop pulmonary lesions during infection (88). Lambs were evaluated and have the potential to serve as an animal model (30).

The purpose of this study was to examine the pygmy goat as a possible animal model for respiratory disease induced by bovine RSV. Histological and ultrastructural data were obtained in an attempt to study events in the pathogenesis of bovine RSV infections.

## CHAPTER 2

### LITERATURE REVIEW

The ultrastructure of the lung has been studied in several mammalian species, including human (20, 58, 72), bovine (3, 39, 40, 91), caprine (7, 57), ovine (63) and porcine (42). With the advent of high resolution electron microscopy, more studies concerning normal and diseased lungs should be undertaken.

#### Bronchi and Bronchioles

The bronchi and bronchioles were composed of a variety of cells, including ciliated and nonciliated cells, goblet cells, brush cells and Clara cells.

The columnar shaped ciliated cells were wider at the luminal surface than at the base and formed complex interdigitations with basal cells, intermediate cells and adjacent cells via desmosomes. An irregular intercellular space surrounded the cells, except at the luminal surface, where tight junctions were formed (49). The cell cytoplasm was not as electron dense as in the nonciliated cells because they were void of secretory products (22).

Organelles found in ciliated cells included rough endoplasmic reticulum, free ribosomes, multivesicular bodies, and occasionally, lysosomes and glycogen (22). Tonofilaments were also found, although they were few in number. Ultrastructurally, they were fine filaments

4-5 nm in diameter, of indefinite length, and served an internal reinforcing function (48). The golgi apparatus was well developed and was located in a paranuclear position. Numerous mitochondria were located beneath the basal bodies to which cilia were attached (22).

Cilia were motile processes, 6-10  $\mu\text{m}$  long and 0.2-0.3  $\mu\text{m}$  in diameter (15, 22). Each cilium was composed of 9 peripheral doublet tubules which surrounded two single central tubules. Located on one tubule of each doublet was a short projection composed of the protein dynein (15).

Atypical cilia have been observed in several disease states (38, 86, 100). Pedersen and Mygind (86) described cilia in which there was a lack of dynein arms on the outer microtubules as well as complete disorganization of the axonemal matrix. Eliasson, Mossberg, Camner and Afzelius (38) observed that an absence of dynein arms in cilia from nasal and bronchial mucosa supported the hypothesis that congenital defects in cilia will cause chronic respiratory tract infections. Sturgess, Chao, Wong, Aspin and Turner (100) revealed cilia with defective radial spokes as a cause of human respiratory disease. They observed cilia from nasal and bronchial biopsies that displayed normal tubules, nexin links, and dynein arms, but lacked radial spokes. In many of the cilia, one of the outer doublet microtubules was displaced into the central region of the axoneme.

Sturgess et al. suggested this displacement of the outer doublet was apparently due to the lack of radial spokes.

The apical border of ciliated cells possessed microvilli (52). Microvilli were cylindrical cell processes 0.5-1  $\mu\text{m}$  long and 80-100 nm in diameter (15, 22). Bundles of straight parallel actin filaments ran longitudinally through the core and occasionally extended into the apical cytoplasm (15). The diameter of these actin filaments was 5 nm (34).

Goblet cells were columnar cells that contained numerous mucous granules and ribosomes. Lower portions of goblet cells were attached to adjacent cells via desmosomes, while luminal intercellular borders were closed by tight junctional complexes. Goblet cells possessed a well developed golgi complex and extensive networks of rough endoplasmic reticulum (22). The surfaces of goblet cells appeared swollen - probably due to accumulated mucin that was about to be released (5). Release of the mucous granules was accomplished by apocrine secretion (50). Microvilli were absent on the swollen surface and were usually more numerous along the cell periphery. These surface microvilli were 0.4  $\mu\text{m}$  long and 0.12  $\mu\text{m}$  in diameter (5).

Rhodin and Dalhamn (87) first described brush cells in the rat tracheal epithelium and noted their infrequent occurrence. Since that time, brush cells have been described by other investigators in tracheal epithelium and epithelium of large and small bronchi (3, 5,



12, 73). Meyrick and Reid (75) described a brush cell in the rat alveolar lining epithelium and felt that if it was observed in other species, it should be called a type III pneumonocyte. Hijiya (55) described proliferation of the alveolar brush cell caused by intraperitoneal injections of bleomycin sulphate. The brush cell was especially prominent in areas of the lung where interstitial pneumonia developed.

The ultrastructure of the brush cell, whether found in tracheal, bronchial or alveolar epithelium, was similar. They were columnar cells which rested on a basement membrane and reached the lumen (22). They contained a dense population of microvilli on the luminal border that were 1-2  $\mu$  long and approximately 0.17-0.25  $\mu$  wide (3, 5, 22, 73). Brush cells contained more cytoplasmic filament bundles than did goblet cells or potential ciliated cells. These cytoplasmic filaments extended from the tips of the microvilli down into the cytoplasm of the cell (3, 5). The function of the brush cell was unknown, although the presence of vacuoles and pinocytic vesicles within the cytoplasm suggested an absorptive function (3, 75, 87).

The epithelium of terminal bronchioles was mainly composed of two cell types - the ciliated cell and the taller nonciliated cell. Clara (28) gave a detailed description of the nonciliated bronchiolar epithelial cell and today these cells are referred to as Clara cells.

Clara suggested that they function as apocrine cells which secrete a nonmucoid substance (98).

Niden (78) proposed that the Clara cell was the major source of pulmonary phospholipid production (presumably surfactant), while the type II alveolar epithelial cell ("large alveolar" cell) possessed phagocytic capabilities and functioned for the clearance of lipids and other materials from the alveoli. Niden suggested the possibility that the phospholipid might be synthesized in the type II cell, but concluded the study demonstrated phagocytic activity of the type II cell and that the radioactive material (tritiated palmitate or acetate) was ingested by the cell as free phospholipid lying in the alveoli.

Azzopardi and Thurlbeck (9) supported Niden's (78) hypothesis that the Clara cell did secrete a phospholipid. They found the Clara cell did not secrete acid mucopolysaccharides, but was rich in choline containing phospholipids in a firmly bound form, probably as a lipoprotein. Cutz and Conen (31) supported Azzopardi and Thurlbeck (9) regarding the cytochemistry and secretory function of Clara cells. Clara cells did contain phospholipid bound to a nonlipid, probably protein, and Cutz and Conen (31) further reported that phospholipid in type II cells was free or loosely bound. Cutz and Conen (31) did not support Niden's (78) suggestion that the type II cell was a phagocytic cell. They believed that a cell metabolically active

toward a secretory function would unlikely be actively phagocytic. The secretions of Clara cells probably made up the hypophase component of the alveolar lining layer and secretions from type II cells contributed to the surface film.

Askin and Kuhn (6) demonstrated that type II alveolar cells (granular pneumocytes) were a major source of dipalmitoyl lecithin, an important component in pulmonary surfactant. Autoradiography led to the conclusion that dipalmitoyl lecithin was not synthesized by Clara cells, and therefore, Clara cells did not function in the synthesis of pulmonary surfactant.

Stinson and Loosli (98) supported the fact that Clara cells possessed a secretory function and provided ultrastructural evidence of secretory activity. Some electron dense granules protruding into the lumen from the surface of Clara cells were enclosed in a uniform, incomplete thin layer of cytoplasm, highly suggestive of merocrine secretion. Other protruding granules were enveloped in a thin cytoplasmic coat, suggesting apocrine secretion. Merocrine secretion involved fusion of the limiting membrane of the secretory granule with the plasma membrane of the cell, and rupture of the membranes with release of the contents into the lumen. Apocrine secretion involves a pinching-off process with release of cytoplasmic buds into the lumen, followed by dissociation of the envelope. Stinson and Loosli (98) proposed both modes of secretion occurred in Clara cells.

Etherton, Purchase and Corrin (46) demonstrated apocrine, not merocrine secretion in Clara cells by utilizing 1-2  $\mu$ m plastic sections stained with hematoxylin and eosin.

Smith, Greenberg and Spjut (95) compared the ultrastructure of the Clara cell in several mammalian species. Membrane bound secretory granules were present in all species, but were sparse in humans and calves. Only in rat secretory granules were crystalloid structures up to 3  $\mu$ m in length observed. Clara cells in mice, rats and rabbits contained abundant smooth endoplasmic reticulum in the apical cytoplasm, whereas human Clara cells contained rough endoplasmic reticulum in parallel cisternae. Glycogen, present in the rabbit and particularly prominent in the calf, was absent in the rat, mouse and human. Only through understanding the comparative ultrastructure can the exact roles of Clara cells be understood in the pathophysiology of the lung (95).

#### Alveolar Epithelium

In 1952 Low (71) described the existence of a pulmonary epithelium and observed that the epithelium completely covered the alveolar walls. Swigart and Kane (101) disagreed with Low (71) and found that the epithelial lining of the alveoli was interrupted. Watrach and Vatter (104) revealed a continuous epithelium composed of two cell types: one cell, was an elongated form possessing long, attenuated cytoplasmic extensions; the other cell, usually large and

polygonal in shape, was located in alveolar niches. Occasionally small invaginations were observed on the inner surface of the cytoplasmic extensions as well as on surfaces of microvilli. The surface of the polygonal shaped cell often displayed microvilli and its cytoplasm contained large opaque bodies which showed irregular laminated internal structures. The junction between two epithelial cells was a narrow space not exceeding 20 nm in width. Watrach and Vatter (104) described a fused basement membrane between the alveolar epithelium and the continuous capillary endothelium which, when near the interstices of the alveolar wall, would separate and follow the alveolar epithelium and the capillary endothelium. Epling (39) supported Watrach and Vatter (104) in that the alveolar epithelial lining was continuous and rested on a basement membrane. He found the majority of the epithelial cells possessed long, thin cytoplasmic processes and occasionally these cells possessed microvilli. Lamellar structures were observed in the cells that bulged into the alveolar lumen and these bulging cells contained numerous microvilli. Epling (39) described epithelial cell junctions as an intercellular space measuring 20 nm. The alveolar epithelium and capillary endothelium possessed their own basement membranes and, in the thinnest part, were separated by a fused basement membrane.

In 1964 Epling (40) described lattice and lamellar structures in the alveolar lumen of normal cattle as well as cattle that had high

mountain disease. He discussed the possibility that these structures might be a result of degenerating epithelial cells due to death, or might be related to the production of surfactant.

Kikkawa, Motoyama and Cook (63) found inclusion bodies in type II alveolar epithelial cells (granular pneumonocytes) that were closely related to surfactant. Inclusion bodies first appeared in lambs around 121 days of gestation and increased in number with increased gestation. Normal surface activity of lung extracts appeared at 126 days of gestation. No laminated or myelin figures were found in alveoli before the appearance of type II cell inclusion bodies. Niden (78) proposed that the type II cells were phagocytic cells and aided in the removal of lipids from the alveoli and were not associated with surfactant production. Dermer (32) found surfactant phospholipid at the surfaces of alveolar epithelial cells, in vesicles contained in the cytoplasm of type I epithelial cells (membranous pneumonocytes) and within basement membranes that separated alveolar epithelium from endothelium. His observations indicated that surfactant was transported away from the alveolar surface during normal turnover and removal of surfactant from the lung. He indicated that junctions between alveolar epithelial cells were tight and surfactant cannot pass into the interstitial space. Dermer (33) found type II cell inclusion bodies to contain a saturated

phospholipid, very similar in structure to that found within emulsions of dipalmitoyl lecithin and isolated surfactant.

Ortega et al. (83) reported that type I alveolar cells usually possessed a smooth plasma membrane in contrast to the type II cell which was covered with numerous microvilli. They observed a close association between type II lamellar inclusions and lysosomal membranes, but strengthened the concept that inclusions were a secretory product of type II cells and not phagocytic structures (65).

Esterly and Faulkner (45) injected ink and polystyrene spheres into the trachea of rabbits and never observed this material in alveolar epithelial cells. They further supported the fact that type II cells were not capable of phagocytic activity.

Nowell and Tyler (80), using scanning electron microscopy, observed microvilli around alveolar type II cells and depressions and openings on their surfaces. These depressions were thought to be directly associated with the discharge of pulmonary surfactant. Atwal (8) described PAS-positive inclusions on the type II cell of the goat and discussed that these inclusions contained mucopolysaccharides which were an important component of pulmonary surfactant. Smith and Ryan (96) obtained evidence that lamellar inclusions of type II alveolar cells were released by merocrine secretion, and that one of the secretory products was tubular myelin. It was this tubular myelin and other phospholipids that other investigators observed

in the alveolar lumen and in laminated inclusions in type II alveolar cells (40, 51, 63, 74, 91, 104). Stratton (99) observed human multilamellar bodies being released by type II cells into the alveolar lumen via merocrine secretion.

Pericytes (cells of Rouget) may be contractile cells that control capillary diameters. Epling (42, 43) described pericytes in direct contact with endothelial cells in lungs and hearts of cattle and swine. They functioned in the regulation of blood flow through vascular beds and might be important chemoreceptors, pressure receptors and thermoreceptors. Atwal and Sweeny (7) observed pericytes in contact with goat alveolar endothelium and in 1974 Weibel (105) observed pericytes associated with capillaries in human lungs. Weibel (105) describes criteria for pericytes: "They are closely opposed to capillary endothelium, are enveloped by its basement membrane, but remain separated from the endothelium by basement membrane leaflets, except in regions where processes approach the endothelial cell, and their processes show a cytoplasmic differentiation similar to that of pericytes".

Alveolar pores were located in thin walls separating adjacent alveoli and were important in providing collateral air circulation and helped prevent the collapse of alveoli if the smaller air passages were blocked (45). Groniowski, Walski and Bicozysko (53) described alveolar pores of Kohn in normal lungs as being a regular oval



circumvallated hole with a diameter of 9  $\mu$ , whereas in collapsed alveoli, the pores had a funnel shaped appearance. Kuhn and Finke (66) observed alveolar pores in the alveolar septa with a diameter of 3-6  $\mu$ . Parra, Gaddy and Takaro (85) found canine alveolar pores about 1  $\mu$ m in diameter and the majority of the pores were covered with material possessing morphologic characteristics of surfactant. Since the pores were covered with surface lining material under normal conditions, they did not participate in providing collateral air circulation. Takaro, Price and Parra (102) found human alveolar pores to have a diameter of 5.3  $\mu$ m if the lungs were perfused via the airway, whereas vascular perfusion produced pores filled with surfactant with an average diameter of 2.6  $\mu$ m.

In a freeze-fracture study Bartels, Oestern and Voss-Wermbter (11) observed communicating junctions between pneumonocytes in humans, dogs, rats, rabbits and mice. Communicating junctions were seen between type I and type II pneumonocytes and between sheets of type I pneumonocytes. They were rarely observed between adjacent type II pneumonocytes. The functional significance of communicating junctions remains open to speculation. The type I pneumonocyte might influence the type II pneumonocyte in the release of surfactant, while the transformation of type II cells into type I cells may be mediated by type I cells adjacent to the type II cells (11).

### Alveolar Damage

In 1964 Epling (41) described alveolar changes associated with acute pulmonary emphysema. Lesions were areas of collapsed alveoli (atelectasis), edematous alveoli, ruptures of the plasma membrane and fibrosis of the alveolar walls.

Epling and Wilson (44) conducted studies concerning ultra-structural changes in pulmonary alveolar necrosis. They observed intracellular edema in type I pneumocytes followed by eventual rupturing of the plasma membrane. This sequence was repeated in endothelial cells. When the plasma membrane of the endothelial cell ruptured, the remaining basement membrane of type I pneumocytes also ruptured, allowing hemorrhage into the alveolar lumen.

Huang, Carlson, Bray and Bradley (57) studied pulmonary lesions caused by 3-methylindole in goats. They observed extensive degeneration and necrosis of type I pneumocytes characterized by mitochondrial swelling, large vesicles and the presence of large clusters of smooth endoplasmic reticulum. The necrosis of the type I pneumocyte was followed by proliferation of the type II pneumocyte in an attempt to repopulate the basal lamina. Bradley and Carlson (21) studied the effects of 3-methylindole in goats on the alveolar epithelium. The most severe morphologic changes were observed in type I pneumocytes and the nonciliated bronchiolar epithelial cells. Type I pneumocytes exhibited swollen vesicles and mitochondria,

large clusters of smooth endoplasmic reticulum, and eventual separation from the basement membrane. Type II pneumonocytes were not as susceptible to injury. They displayed slightly swollen mitochondria with mild cytoplasmic swelling.

Evans, Dekker, Cabral-Anderson and Freeman (47) demonstrated that a greater proliferative response of alveolar type II pneumonocytes was associated with increasing tissue damage after exposure to nitrous dioxide ( $\text{NO}_2$ ). Following proliferation, the type II pneumonocytes differentiated into type I pneumonocytes and the epithelium assumed a normal squamous appearance.

Castleman, Dungworth, Schwartz and Tyler (24) studied the pathogenesis of acute respiratory bronchiolitis in rhesus monkeys after exposure to ozone. They observed extensive degeneration and necrosis of type I pneumonocytes. The type II pneumonocytes functioned as stem cells in renewal of the epithelium.

Adamson and Bowden (1) showed type II pneumonocytes were susceptible to injury. In a steady state, type II pneumonocytes were considered to be injury resistant, whereas in a proliferative phase, after necrosis of type I pneumonocytes, type II pneumonocytes were not resistant to injury.

Langloss, Hoover and Kahn (67) studied the ultrastructural morphogenesis of acute viral pneumonia in cats produced by a virulent strain of feline calicivirus. In type I pneumonocytes there was

dilatation of mitochondria, chromatin was clumped and margined and partial detachment of cytoplasmic extensions eventually led to complete desquamation. Many severely affected type I pneumonocytes contained aggregates of viral particles. Type II cells displayed some degenerative changes and often remained in situ after the loss of type I pneumonocytes. During the reparative phase the respiratory membrane was thick due to hyperplasia of type II pneumonocytes. This hyperplasia of type II cells was not considered to be viral specific, but represented a nonspecific response to type I cell injury.

#### Respiratory Syncytial Virus

In 1956 Morris, Blount and Savage (77) isolated a virus from a chimpanzee that displayed signs of respiratory disease - coughing, sneezing and a mucopurulent discharge. This virus, the chimpanzee coryza agent (CCA), produced degenerative changes in cell cultures, was not pathogenic for common laboratory animals and remained pathogenic for chimpanzees. A laboratory worker working with CCA developed an upper respiratory illness characterized by rhinorrhea, cough, malaise and a low grade fever. Serological studies on the worker provided a 1:80 complement fixation titer and a 1:40 neutralizing antibody titer against CCA. This evidence was presumptive that CCA was of etiological significance.

In 1957 Chanock, Roizman and Myers (25) isolated from humans an agent indistinguishable from the CCA. This new isolate along with

the CCA were called respiratory syncytial (RS) viruses due to their antigenic properties and characteristic syncytium formation in tissue cultures. Since then, the RS virus has been shown to be the most important respiratory tract pathogen during early life (13, 26, 27).

Paccaud and Jacquier (84) were the first to isolate a bovine respiratory syncytial virus from an outbreak of respiratory disease in Switzerland. The infection spread to all cattle less than 6 years of age. Young animals developed an upper respiratory tract infection with cough and nasal discharge while older animals displayed signs of bronchopneumonia. Attempts to detect hemagglutinating and hemadsorbing activity with this virus failed.

Smith, Frey and Dierks (92, 93) were the first to isolate a bovine respiratory syncytial virus in the United States. In a serological survey, 81% of Iowa cattle tested possessed serum antibody to the bovine isolate. They reproduced clinical disease in three of five calves tested. Clinical signs noted were anorexia, pyrexia, nasal discharge and malaise. In all calves a leukopenia was noted three to five days after infection.

Rosenquist (90) isolated a respiratory syncytial virus from calves with acute respiratory disease in Missouri. The respiratory disease was characterized by polypnea and fever. A few calves displayed a mucopurulent nasal discharge and some calves had a serous nasal discharge. Rectal temperatures averaged 104.7° F.

Recently Smith, Lehmkuhl and Phillips (94) isolated a respiratory syncytial virus from a herd of pygmy goats that displayed signs of respiratory disease. Clinical signs in infected goats included elevated temperatures, anorexia, malaise, cough, mucopurulent nasal discharge and purulent lacrimal discharge with photophobia. The morphogenesis and ultrastructure of this isolate provided additional evidence that it was a respiratory syncytial virus.

#### Ultrastructure of Respiratory Syncytial Virus

##### Negatively Stained Preparations

Bloth, Espmark, Norrby and Gard (16) used the Long strain of the RS virus to obtain information about its ultrastructure. They reported on the great pleomorphism of the virus - many virions appeared spherical, while others were more or less elongated. The diameters of the virions ranged from 90-860 nm with an average of 340 nm. Virions possessed surface projections which covered the entire particle. These club-shaped projections had a length of 13-17 nm and a width of 4-7 nm. The center to center distance between projections was 7-10 nm.

In a later study Bloth and Norrby (17) reported on the ultrastructure of RS virus subunits. They observed two different types of viral structures. One type had a rosette-like shape with diameters of 50-75 nm and an average about 60 nm. The rosettes were the dominant particle and possessed spikes with lengths of

12-16 nm. The second type of structure came from particles that had been disrupted by treatment with Tween 80. These helical structures were fragile and had diameters of 10-12 nm and a regular periodicity along its axis of 7 nm. Eckert, Maassab and Cavallaw (36) also described the inner component of RS virus as being a helical structure which varied in diameter between 13-18 nm. Although large, elongated virions predominated, spherical particles with average diameters of 150 nm were also observed. Both forms of the virus were covered with surface projections. Bloth and Norrby (18) repeated their studies on the internal component of the RS virus because of the distortion obtained in the preparation of materials (17). They observed the inner structure leaking out from disrupted virions as long strands. These strands reached lengths more than 1.5  $\mu$  with diameters of 16-18 nm. The RS virus internal component had a herringbone-like structure with a regular periodicity of 7 nm along its axis.

Joncas, Berthiaume and Pavilanis (61) studied the fine details of an RS virus isolated from nasopharyngeal secretions of three infants with bronchiolitis. The viral particles were spherical, filamentous and pleomorphic, varying in diameters from 80-500 nm. Spherical forms varied in diameter from 100-350 nm. Surface projections measuring 15 nm were observed on the surface of the RS virus. The nucleoprotein strand varied in diameter from 12.5-15 nm with an

average of 13.5 nm and a helical pitch of 6.5 nm. Ito, Tanaka, Inaba and Omori (60) examined an RS virus that was isolated earlier in Japan (59). The RS virus exhibited great pleomorphism - some spherical and some elongated or distorted. The diameters varied from 80-450 nm with an average of 200 nm. An outer membrane 7-15 nm thick was covered by club-shaped projections 13-17 nm long and 4-7 nm wide with a center to center distance of 7-9 nm. The internal structure of disrupted virions had herringbone-like strands 11-15 nm wide and a regular periodicity of 7 nm. When utilizing negative staining techniques, Backi and Howe (10) observed filamentous and spherical virions. Filaments measuring 1-4  $\mu\text{m}$  predominated while occasionally spherical virions with diameters between 150-500 nm were seen. Both forms possessed surface projections which measured 10 nm in length. Berthiaume, Joncas and Pavilanis (14) also observed the RS virus in negative stained preparations. The RS virus contained a nucleocapsid core surrounded by an envelope covered with projections. These surface projections measured 12 nm in length with a center to center spacing of 10 nm. The nucleocapsid had an average diameter of 13.5 nm with a helical pitch of 6.5 nm - the nucleocapsid of the RS virus was a fragile structure and was broken into small fragments and isolated rings. Lehmkuhl, Smith and Cutlip (69) studied the structure of a caprine RS virus isolated by Smith et al. (94). Pleomorphic, spherical and filamentous structures were observed in



negatively stained preparations with filamentous forms predominating. The filamentous forms had diameters ranging from 45-90 nm with lengths up to 2,000 nm, while spherical forms had diameters ranging from 80-600 nm. The envelope possessed club-shaped projections 10-14 nm long with a center to center spacing of 8-11 nm. The nucleocapsid was a fragile structure observed as broken fragments or isolated rings.

#### Ultrathin Sections of Respiratory Syncytial Virus

Norrby, Marusyk and Orvell (79) infected Vero cells with the Long strain of RS virus for ultrastructural studies. Cytoplasmic inclusion bodies had a granular or threadlike appearance. Occasionally filamentous structures with dimensions of the RS virus were seen in association with inclusion bodies. Virus maturation occurred at the plasma membrane. Spherical particles with four to five (occasionally 10 to 12) submembranous dots were seen budding from the plasma membrane. These distinct dots had diameters of 11-15 nm, while the spherical particle ranged from 90-130 nm in diameter. Surface projections with lengths of 12-15 nm were observed on the spherical particle. Filamentous or elongated structures were also seen extending from the plasma membrane. Occasionally the distinct dots were associated with these filamentous structures. The filamentous forms had a uniform diameter of

100-130 nm with their lengths occasionally exceeding 2  $\mu$ m. The tips often had the appearance of a budding virion.

Ito et al. (60) also demonstrated viral maturation occurring at the plasma membrane in the form of spherical and filamentous structures. The spherical particles ranged from 80-130 nm in diameter with distinctive dots of 11-15 nm. They speculated that these dots might be cross sections of filamentous components. The filamentous virions were of variable length with diameters of 100-130 nm.

Bachi and Howe (10) observed round to kidney-shaped and filamentous structures budding from the plasma membrane of virus infected cell cultures. Spherical particles with diameters of 150-250 nm frequently contained electron dense dots with a diameter of 15 nm. Budding filaments with diameters of 90-100 nm did not contain distinct dots but contained three to five parallel strands measuring 15 nm in diameter. Coreless filaments and spheres were frequently observed budding from the cell surface. Berthiaume et al. (14) observed RS virus budding from the plasma membrane of infected cell cultures. They could not observe the first stages of adsorption and penetration of the virus due to the relatively low multiplicity of infection. Cytoplasmic inclusion bodies were localized in a paranuclear position and had a granular or thread-like appearance. These threads had a diameter of approximately 12 nm.

Spherical and filamentous particles with a uniform diameter of 100 nm were seen budding from the plasma membrane. Both structures possessed surface projections approximately 12 nm in length. Electron dense dots varying in number from 4 to 8 with a diameter of 12 nm were seen in spherical particles. The filamentous particles contained 3-4 parallel elongated threads approximately 12 nm in diameter.

Lehmkuhl et al. (69) observed spherical and filamentous particles maturing at the plasma membrane. Granular, pleomorphic cytoplasmic inclusions were located in a paranuclear position. The spherical and filamentous particles possessed diameters of 90-160 nm. Spherical virions possessed electron dense dots with diameters of 11-15 nm, whereas in longitudinal sections these dots appeared as filaments. Occasionally some of the filamentous virions had a terminal swelling.

#### Pathological Changes

The RS virus has been established as an important cause of severe respiratory disease and death in children, especially those children under one year of age (4, 13, 26, 29, 37, 56).

Aherne, Bird, Court, Gardner and McQuillin (2) described pathological changes in children caused by the RS virus. RS virus was recovered from the lungs of 12 children at autopsy. Five of these children showed histological changes of acute bronchiolitis - necrosis of the bronchiolar epithelium followed by lymphocytic

infiltration with some plasma cells and macrophages. The sub-mucosa was edematous and typically, there was no damage to muscle and elastic fibers. Thick dense plugs also formed in the bronchiolar lumen and consisted of cell debris, fibrin and a material that stained similarly to DNA. Cytoplasmic inclusion bodies were difficult to locate in the pre-necrotic bronchiolar epithelium.

Richardson et al. (88) described lesions in the lungs of cebus monkeys caused by a respiratory syncytial virus. The alveolar septa were thickened due to an infiltration of mononuclear cells and polymorphonuclear leukocytes (PMNs) while multinucleated giant cells were occasionally observed in the alveoli. Eosinophilic cytoplasmic inclusion bodies were observed in areas of consolidation six days after experimental infection.

Mohanty, Ingling and Lillie (76) described histological changes in calves induced by RS viral infection. The alveolar septa were thick due to a mononuclear infiltration. Multinucleated giant cells were seen in the alveolar lumen and neutrophilic infiltrations were observed in alveolar spaces. The bronchiolar lumens were partially occluded with neutrophils and cellular debris. Lymphocytic and reticuloendothelial hyperplasia was noted in bronchial lymph nodes and neutrophils were observed in lymph sinuses.

Bryson, McFerran, Ball and Neill (23) described lesions in calves from naturally occurring RS and parainfluenza infections. The

bronchiolar lumen was occluded with an exudate consisting of mononuclear cells, PMNs, detached epithelial cells and proteinaceous debris. PMNs were observed within bronchial and bronchiolar epithelium and in the lamina propria. The lamina propria of small bronchi contained increased numbers of plasma cells and lymphocytes. The alveolar septa were thickened due to edema and an increased content of interstitial cells. PMNs, macrophages and monocytes were present in many alveolar lumens. Multinucleated giant cells with eosinophilic cytoplasmic inclusions were seen on bronchiolar and alveolar walls in some of the infected animals.

Lehmkuhl and Cutlip (68) described lesions in lambs induced by the RS virus. All lobes of the lung displayed multiple foci of interstitial pneumonitis. The alveolar septa were thickened due to an accumulation of mononuclear cells with the macrophage being the predominant cell type. Cutlip and Lehmkuhl (30) described lung lesions in lambs experimentally infected with RS virus. The main lesion was of a focal interstitial pneumonitis with multiple areas of consolidation. Histologically the alveoli and alveolar septa had an extensive accumulation of macrophages. Many type II pneumocytes were hyperplastic, forming a cuboidal epithelial lining. The terminal air passages displayed necrosis and sloughing of epithelial cells. Multinucleated giant cells were rarely observed and no cytoplasmic inclusion bodies were observed in H&E or Giemsa

stained sections. Utilizing the electron microscope, they observed pleomorphic virions budding from small airway epithelial cells and free virions in small airways and alveoli. Dense cytoplasmic inclusions located in a paranuclear position were observed in several epithelial cells.

The respiratory syncytial virus has recently been placed in the genus Pneumovirus of the family Paramyxoviridae (64) and has been established as an important pathogen of early life (4, 13, 26, 27, 29). Few studies have been conducted at the ultrastructural level during experimental or natural infection and more work is desired in this area.

## CHAPTER 3

### MATERIALS AND METHODS

#### Cell Culture and Culture Media

Georgia Bovine Kidney (GBK) cells were used for virus propagation and titration. The cells were maintained in Dulbecco's Modified Eagle Medium (DMEM) with 10% fetal calf serum at pH 7.2. Five ml of the cell suspension were used to seed each 250 ml plastic tissue culture flask.<sup>1</sup> The flasks were placed in an incubator with 5% CO<sub>2</sub> at 37° C. Confluent monolayers were obtained after one day incubation.

#### Stock Virus

Missouri isolate VC484, a bovine respiratory syncytial virus, was propagated in GBK cells for 4-6 days or until 50-60% of the cell monolayer displayed signs of cytopathic effect (CPE) - cell rounding, aggregation and sloughing. Prior to freezing at -70° C a solution of sucrose, phosphate and glutamate (SPG) was added to the medium following the method of Bovarnick, Miller and Snyder (19). The virus suspension remained frozen until needed for experimental infection in pygmy goats.

---

<sup>1</sup>Costar, Division Data Packaging Corp., Cambridge, Mass.

Control Inoculum

The control inoculum consisted of GBK cells maintained in DMEM with 10% fetal calf serum. SPG was added to the medium prior to freezing at  $-70^{\circ}$  C.

Virus Titration

VC484 was titered using tissue culture plates containing 24 wells.<sup>2</sup> Each well contained a monolayer of GBK cells. The growth medium was removed from the wells and the cells rinsed with Rinaldini enzyme solution (R-saline). Each well was inoculated with 0.2 ml of five-fold virus dilutions made in DMEM without serum. Adsorption was allowed for one hour in a moist atmosphere at  $37^{\circ}$  C. After adsorption, the dilutions were removed and the monolayers overlaid with 0.5% agarose in DMEM. After incubation for 5-6 days or until adequate CPE was noted with an inverted microscope, the monolayers were fixed at room temperature for 30 minutes with 10% buffered neutral formalin. Agar plugs were removed and the monolayers stained with crystal violet. Plaques were counted in each well to determine the number of plaque forming units (PFU). Calculations were then made to determine the number of PFU per ml of stock virus. Titrations were done in quadruplicate. The titer of VC484 was  $1.5-2.0 \times 10^6$  pfu/ml.

---

<sup>2</sup>Falcon Plastics, Oxnard, Calif.



Pygmy Goats

African pygmy goats, raised by Dr. M. H. Smith at the Veterinary Research Laboratory, Montana State University, Bozeman, Montana, were used in this study. Five goats were used to study normal lung structure, five were infected with bovine RSV and two utilized as controls for virus infection.

Five goats, ages 6 months to 3 years, were selected at random and used for normal lung structure. Five goats, ages 6-8 months were randomly selected and infected with a bovine RSV. Goats were anesthetized according to manufacturers instructions using Ketamine HCl<sup>3</sup> and small animal Rompun<sup>4</sup> given intramuscularly. Fifteen ml of stock virus was aerosolized into the nasal cavity using a disposable DeVilbiss<sup>5</sup> nebulizer and five ml was injected into the trachea. Goats were euthanatized six, seven and nine days after virus challenge. Two goats ages 6-8 months utilized as control goats were anesthetized as were the RSV goats and given the control inoculum as previously described. These two goats were euthanatized six days after challenge. All goats were euthanatized in a humane manner using 10 ml of 10%

---

<sup>3</sup>Bristol Laboratories, Syracuse, N.Y.

<sup>4</sup>Cutter Laboratories, Inc., Shawnee, Kan.

<sup>5</sup>DeVilbiss Co., Somerset, Penn.

Surital<sup>6</sup> administered intravenously. Immediately after death the thoracic cavity was opened and the lungs removed for fixation.

#### Fixation

Lungs from eleven goats were fixed as described by Dungworth, Schwartz and Tyler (35) utilizing airway perfusion. A modification concerning the buffer was made. Cacodylic acid<sup>7</sup> was used instead of sodium cacodylate. The pH was adjusted to 7.2-7.3 using 1N NaOH with a molarity of 0.2 M. Lungs were inflated via the trachea using a glutaraldehyde/paraformaldehyde fixative at 30 cm of fluid pressure. The lungs were totally immersed in the fixative bath during this procedure. After fixation at room temperature for 12-20 hours, the lungs were removed from the fixative bath and prepared for light and electron microscopy. The lung from one RSV infected goat was removed from the thoracic cavity and immediately processed for microscopy without using tracheal perfusion.

#### Light Microscopy

Tissue was removed from the apical and right diaphragmatic lobes and placed in 10% buffered neutral formalin (BNF) for a minimum of 24 hours. Following fixation all tissues were stained with hematoxylin and eosin and were examined using a Leitz microscope.

---

<sup>6</sup> Parke-Davis, Morris Plains, N.J.

<sup>7</sup> Polysciences, Inc. Warrington, Penn.

Photomicrographs were taken using a Zeiss standard universal microscope on 4x5" format.

### Electron Microscopy

#### Transmission Electron Microscopy (TEM)

Tissues taken from the apical and right diaphragmatic lobes were minced into 1 mm cubes and post-fixed for 2 hours in 1%  $\text{OsO}_4$  in 0.1 M cacodylate buffer with a pH of 7.2-7.3. They were then placed in 0.1 M cold cacodylate buffer and washed three times, 15 min. each. Tissue taken from the animal without tracheal perfusion was diced into 1 mm cubes and placed into 2%  $\text{OsO}_4$  in 0.1 M cacodylate buffer, pH 7.2-7.3, for two hours. After fixation with 2%  $\text{OsO}_4$  the tissue was washed in 0.1 M cacodylate buffer as described above. All tissues were then dehydrated stepwise in 50, 70, 95 and 100% ethanol. The tissue was infiltrated with Spurr's epoxy resin (97) and polymerized at 70° C for 15 hours in size 00 BEEM capsules.

Eight to ten blocks of tissue were sectioned from each goat using glass knives on a Reichert OM-U2 ultramicrotome. Only sections 50-100 nm thick, as judged by interference colors, were placed on 3 mm copper grids of 200 mesh. Thin sections were then stained for 5 min. with uranyl acetate and for 3-5 min. in Reynolds lead citrate (70). Grids were then examined using a Zeiss EM 9S-2 or a JEOL 100 CX transmission electron microscope at 60-100 KV.

### Scanning Electron Microscopy (SEM)

Tissue fixed in the glutaraldehyde/paraformaldehyde fixative, approximately 8x3x3 mm, was used for scanning electron microscopy. Tissue blocks were first washed with water and then dehydrated stepwise in 30, 50, 70, 90, and 100% ethanol. The tissue was then dried by the critical point drying system using CO<sub>2</sub> (82). Dried tissue was mounted on copper SEM stubs using colloidal graphite and then sputter coated with gold.

Tissue was examined using a JEOL 100 CX with an ASID-4D scanning attachment at 40 KV.

### Electron Microscopy of Particle Suspensions

The method of Ritchie and Fernelius (89) was used to assure the presence of BRSV in viral cell cultures. Stock pools of virus were centrifuged at low speed to pellet cells, cell debris and virus. The supernate was discarded and the pellet resuspended in a few ml of distilled water. Four to six drops of the suspension were added to a spot well containing two drops of 4% phosphotungstic acid, two drops of a freshly prepared 0.3% suspension of bovine serum albumin and 15-30 drops of distilled water. The resulting solution was mixed in a pipette and placed into an all-glass nebulizer.<sup>8</sup> The preparation

---

<sup>8</sup> Ted Pella Inc., Tustin, Calif.

was sprayed onto a carbon coated formvar filmed grid and immediately examined using a JEOL 100 CX transmission electron microscope operated at 80-100 KV.

#### Electron Microscopy of RSV Infected Cell Culture

Respiratory syncytial virus infected bovine turbinate cells were propagated in a 250 ml plastic flask. The method described by Ushijima (103) was used for fixation, dehydration and embedment of tissue cultures for use in electron microscopy.

The cells were washed with R-saline and trypsin was added to release the cells from the surface of the flask. Two ml of 10% fetal calf serum was added to each flask. The cell suspension was centrifuged at 1,000 rpm for 10 minutes in a refrigerated centrifuge with a swinging bucket rotor #269.<sup>9</sup> The pellet was washed with .06 M Sorenson's phosphate buffer pH 6.4-6.5 and again centrifuged at a low speed for 10 minutes. The pellet was fixed for 1 hour at 4° C in 4% glutaraldehyde in .06 M Sorenson's phosphate buffer to which was added 0.85% NaCl. The suspension was centrifuged at 1,000 rpm for 10 minutes and 1-2 ml of 1% agarose was added to each pellet. The pellet was resuspended in agarose and placed on a glass slide to cool and solidify. The solid was cut into 1 mm cubes and washed

---

<sup>9</sup>International Equipment Co., Boston, Mass.

3 times in Sorenson's phosphate buffer. Cubes were post fixed in 1%  $\text{OsO}_4$  in Sorenson's buffer for 1½-3 hours at 4° C. Cubes were washed three times in Sorenson's buffer, dehydrated in an ethanol series and embedded in Spurr's epoxy resin. Polymerization occurred in 15 hours at 70° C. Ultrathin sections were examined using a Zeiss EM 9S-2 transmission electron microscope operated at 60 KV.

## CHAPTER 4

### RESULTS

#### Clinical Signs

There were no apparent clinical signs of disease in pygmy goats infected with bovine RSV.

#### Negatively Stained RS Virions

Negative staining techniques applied to RSV infected bovine turbinate cell cultures revealed spherical, filamentous and pleomorphic virions. Spherical virions measured 140-177 nm in diameter and filamentous virions were approximately 50-70 nm wide. Both forms were completely covered with club-shaped surface projections with diameters ranging from 4-6 nm, lengths of 12-17 nm and a center to center spacing of 5-10 nm (Figs. 1, 2). Rosette-shaped virions approximately 100-110 nm in diameter were completely covered with surface projections (Fig. 3). Pleomorphic virions possessed hexagonal arrays of surface projections. The diameter of individual projections ranged from 4-5 nm. The terminal ends of these projections appeared to be in close proximity to adjacent projections, and in some cases appeared to be making direct contact with adjacent projections (Figs. 4, 5).

Bovine Turbinate Cell Culture Infected With RSV

Respiratory syncytial virus maturation occurred at the plasma membrane. Large pleomorphic cytoplasmic inclusion bodies (or possibly lysosomes) were located in paranuclear positions in infected cells (Fig. 6). Spherical and filamentous virions budded from the plasma membrane. Spherical virions were 133-151 nm in diameter and contained peripheral submembranous electron-dense dots. The dots varied in diameter from 11-16 nm. Filamentous virions varied in width from 111-150 nm and possessed two parallel strands or electron-dense dots. The parallel strands were 11-14 nm wide and the electron-dense dots varied in diameter from 11-16 nm. Both the spherical and filamentous virions possessed well-developed peripheral surface projections (Fig. 7).

Normal Goat Lung

The alveolar septa appeared thin and alveoli were clear of macrophages, red blood cells and cell debris (Fig. 8). Respiratory bronchioles led into alveolar ducts which branched into alveolar sacs (Fig. 9). Adjacent to respiratory bronchioles were numerous alveoli which displayed pores of Kohn (Fig. 10).

The epithelial lining of alveoli was composed of two cell types - membranous or squamous alveolar epithelium (type I pneumonocytes) and the granular alveolar cell (type II pneumonocyte). Sparse microvilli were observed on the surface of type I pneumonocytes, whereas



the bulging type II pneumonocyte was densely covered with surface microvilli. The raised areas between the large flat sheets of type I cells were marginal folds. Pores of Kohn provided for collateral air circulation (Fig. 11). There were well-demarcated junctions between type I and type II pneumonocytes. Microvilli on type II pneumonocytes varied considerably in length (Fig. 12).

The lung was a highly vascular organ that contained many capillary beds. The bulges in alveolar walls depicted capillary locations and contained red blood cells, nuclei of endothelial cells, or nuclei of type I pneumonocytes (Fig. 13).

The nonciliated bronchiolar epithelial cell (Clara cell) possessed microvilli and secretory blebs. These blebs ruptured and released their contents (surfactant) into the lumen of the bronchioles. Clara cells were adjacent to other nonciliated cells and ciliated cells. These ciliated cells also possessed numerous microvilli (Figs. 14, 15).

Ultrathin sections misleadingly depict type I pneumonocytes with a relatively smooth surface free of microvilli or surface projections while scanning micrographs reveal microvilli (Figs. 11, 12). They possessed their own intact basement membrane which may fuse with basement membranes of underlying endothelial cells. The long slender projections of type I pneumonocytes occupied more surface area than

did cuboidal type II pneumonocytes. Type I cells also possessed many caveolae which form small pinocytotic vesicles (Figs. 16, 17, 18).

Type II pneumonocytes possessed surface microvilli, numerous glycogen granules and mitochondria, and small to large vesicles that appeared empty or occasionally contained lamellar structures. Microvilli varied in diameter ranging from 80-130 nm and possessed actin filaments 6-8 nm in diameter. Tight junctions were observed on the luminal surface connecting type I and type II pneumonocytes (Figs. 19, 20).

In bronchioles, Clara cells and other nonciliated cells possessed a homogeneous electron dense cytoplasm. Clara cells contained numerous glycogen granules and secretory droplets. The secretory droplets were mainly located in the apical portion of the cytoplasm near the plasma membrane. Occasionally secretory droplets were observed being released from Clara cells via merocrine type secretion. Both Clara cells and nonciliated cells possessed microvilli ranging from 100-130 nm in diameter with 6-8 nm filaments (Figs. 21, 22).

Ciliated cells in terminal bronchioles possessed surface microvilli with electron-dense dots, glycogen granules, few mitochondria and a cytoplasm that was homogeneous in regard to electron density. The actin filaments were 6-9 nm in diameter while the glycogen

granules ranged from 19-26 nm. Cilia were attached to the cell by means of basal bodies (Figs. 23, 24).

Cilia possessed typical axonemes. The plasma membrane was composed of a trilaminar structure approximately 13 nm in diameter. Nine peripheral doublet tubules surrounded two central tubules. One tubule of each peripheral doublet had a dynein arm and spokes radiated from the doublets toward the central tubules (Fig. 25).

#### RSV Goat Lung

Bovine RSV caused changes in the structure of goat lungs. The alveolar septum was thickened in two goats. The thickening was due to fibrosis as well as the infiltration of monocytes and PMNs into the alveolar connective tissue. The capillaries were congested and macrophages were occasionally observed free in the alveolar lumen (Fig. 26).

One goat had a peribronchiolar infiltrate with normal adjacent alveoli. Monocytes were the characteristic cell type although a few PMNs were observed infiltrating the lamina propria and between adjacent epithelial cells in terminal bronchioles (Figs. 27, 28).

Several changes occurred in large bronchi of RS virus infected goats. The pseudostratified ciliated columnar epithelium was necrotic. Lymphocytes and PMNs migrated between the epithelial cells toward the lumen and the lamina propria was edematous. A bronchial plug was observed in the lumen of one goat. The plug consisted of

cellular debris, macrophages, lymphocytes and occasional PMNs and eosinophils (Figs. 29-31).

Type II pneumonocytes contained secretory blebs and secretory pits with surfactant protruding from pits. They were located adjacent to type I cells with numerous surface projections. Merocrine secretion was observed in type II pneumonocytes (Figs. 36, 37).

Goblet cells in bronchioles possessed secretory blebs covered with microvilli. These mucus containing cells were adjacent to ciliated cells. There did not appear to be a loss of cilia associated with RS viral infection (Fig. 38).

Type I alveolar pneumonocytes displayed a hyperplasia of surface projections including budding filamentous RS virions (Figs. 32-35, 39). Some type I cells had increased electron density beneath the plasma membrane. Cytoplasmic inclusion bodies (or possibly lysosomes) were located in a paranuclear position (Fig. 40). Similar structures were not observed in normal or control goat sections.

Filamentous and spherical RS virions were observed budding from the surface of type I pneumonocytes. Occasionally well-developed surface projections were seen on filamentous virions. These surface projections were 19-25 nm long and had a club-shaped head 6-8 nm in diameter. Electron dense dots were observed in spherical virion and measured 10-14 nm in diameter. The spherical virions had diameters of 80-100 nm (Figs. 41-43).

Respiratory syncytial virus maturation also occurred at the plasma membrane of type II pneumonocytes and these type II cells retained secretory activity. Spherical as well as filamentous virions budded from the plasma membrane. Spherical virions measured 100-150 nm in diameter and possessed 13-15 nm electron-dense dots. Filamentous virions varied in length, had diameters of 100-130 nm and contained electron-dense dots 13-16 nm in diameter (Figs. 44-48). Mitotic type II cells were not observed.

Nonciliated cells in bronchioles possessed spherical and filamentous RS virions. Filamentous virions reached lengths up to 1  $\mu$ m with diameters ranging from 120-150 nm. Parallel strands 13-15 nm in diameter were observed in some of the filamentous virions. Other filamentous virions contained electron-dense dots measuring 13-15 nm. Spherical virions budding from the plasma membrane measured 100-150 nm in diameter and had electron-dense dots 11-13 nm. Many electron dense areas beneath the plasma membrane were also observed (Fig. 49, 50).

Ciliated cells in terminal bronchioles possessed filamentous RS virions projecting from the plasma membrane. Some of the virions possessed terminal swellings and a few appeared to branch. The virions varied in length and diameter. Diameters ranged from 100-160 nm. One virion possessed a terminal swelling measuring 230 nm in diameter, and a structure with projections measuring 140-147 nm

was located inside the terminal swelling (Fig. 51). This structure of 147 nm with its projections was very similar to the rosette-shaped RS virion observed in a negative stained cell culture preparation (Fig. 3).

#### Control Goat Lung

Large bronchi did not possess cellular plugs and terminal bronchioles were not involved in an inflammatory response. The alveolar septa were thin and alveoli were not congested (Fig. 52).

Type I pneumonocytes appeared as large flat sheets of thinly attenuated cytoplasm and possessed microvilli. The microvillous covering was not as dense as observed in lungs infected with RSV, but appeared similar to those observed in normal lungs. Alveolar pores of Kohn were variable in size (Fig. 53).

Type II pneumonocytes actively produced surfactant. Many type II cells possessed secretory blebs and pits and surface lining material was observed being discharged from secretory blebs. Microvilli of various lengths protruded from the surface of type II cells (Figs. 54, 55).

Respiratory bronchioles contained Clara cells, as well as other nonciliated and ciliated cells lining their surface. Clara cells possessed surface microvilli and large secretory blebs. Adjacent to Clara cells were other Clara cells, nonciliated or ciliated cells. Both the nonciliated and ciliated cells possessed surface microvilli.

The junction separating respiratory bronchioles from alveoli was abrupt, and Clara cells were observed adjacent to type I pneumocytes (Figs. 56, 57).

In large bronchioles, goblet cells were adjacent to nonciliated and ciliated cells. Both goblet cells and nonciliated cells possessed dense peripheral microvilli. The microvilli on the nonciliated cell appeared longer than microvilli on goblet cells (Fig. 58).

Clara cells, possessing surface projection of various shapes, release their secretory product via merocrine secretion. Numerous mitochondria and secretory droplets were located in the apical portion of the cytoplasm. Glycogen granules were abundant throughout the cytoplasm. The electron density of secretory droplets differed from the material that was about to be released into the lumen. The extruding material was less electron dense than secretory droplets. Surface active material was observed in the lumen of bronchioles (Figs. 59, 60).

Brush cells were occasionally seen in bronchioles. Microvilli of brush cells were much coarser than microvilli of type II pneumocytes. Long, streaming filaments extended from the cytoplasm of the microvilli down into the apical portion of the cell. Brush cells were connected to adjacent cells at the luminal surface via tight

junctions. The lateral portions of the cell were connected to adjacent cells by desmosomes. Brush cells were observed only in bronchioles and not in the alveolar wall (Fig. 61).

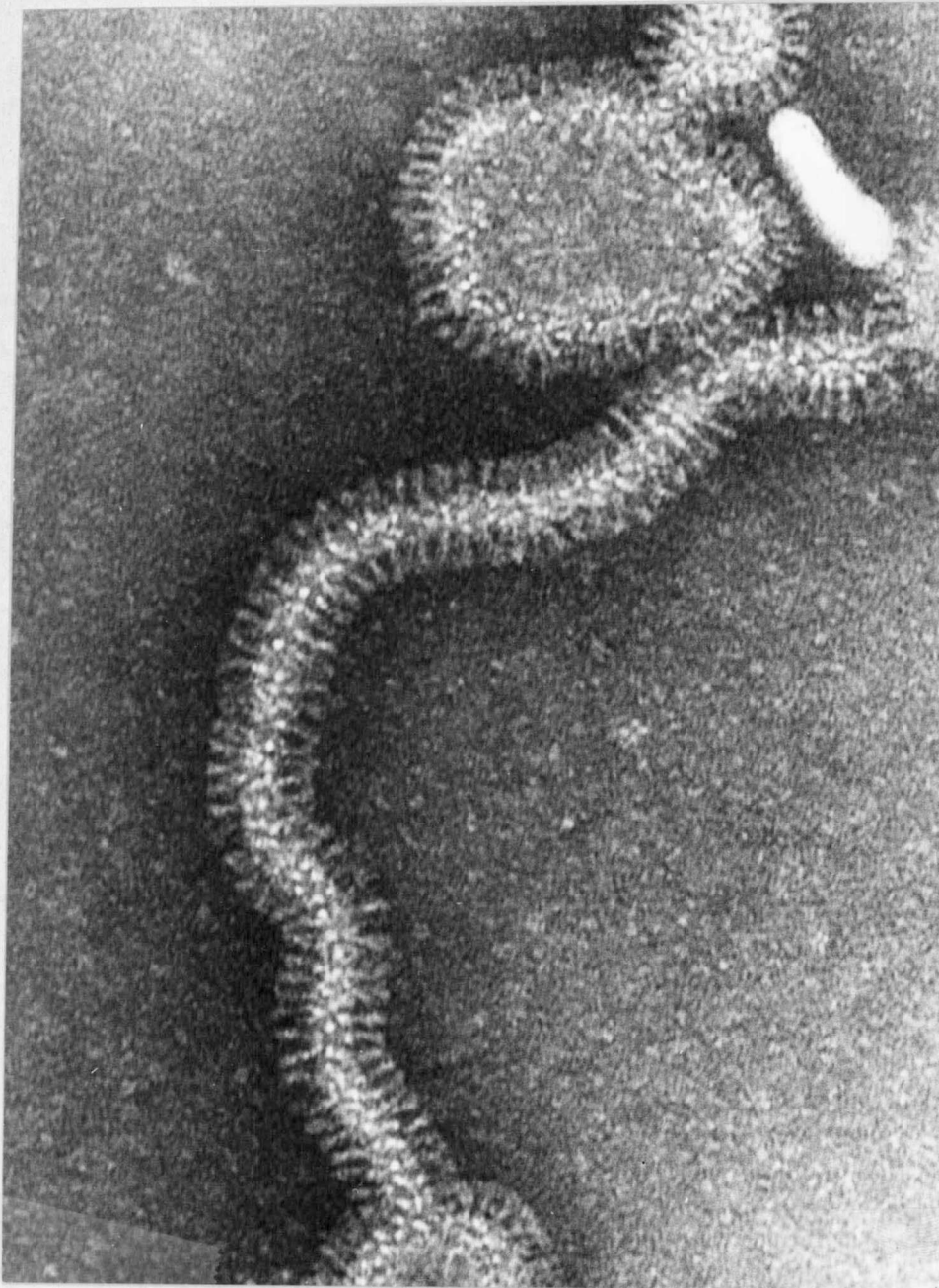
#### Comparative Distribution of Microvilli

Random scanning micrographs of type I pneumonocytes were taken of normal, RS virus infected and control goats. Type I pneumonocytes in normal and control goats possessed sparse surface microvilli (Figs. 62, 63). Type I cells of RS virus infected goats possessed numerous microvilli with a possibility that many of the surface projections were RS virions (Fig. 64).





Fig. 1. Negatively stained spherical and filamentous RS  
virions. X300,000.



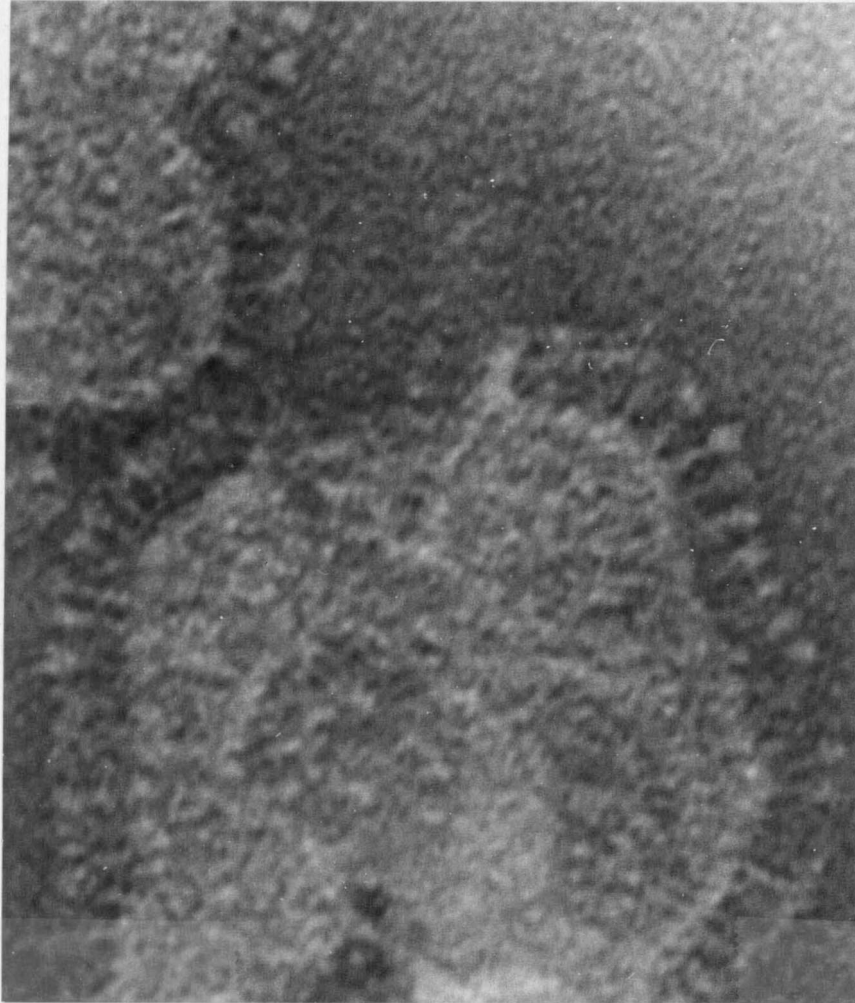


Fig. 2. Negatively stained spherical RS virion showing club-shaped surface projections. X750,000.

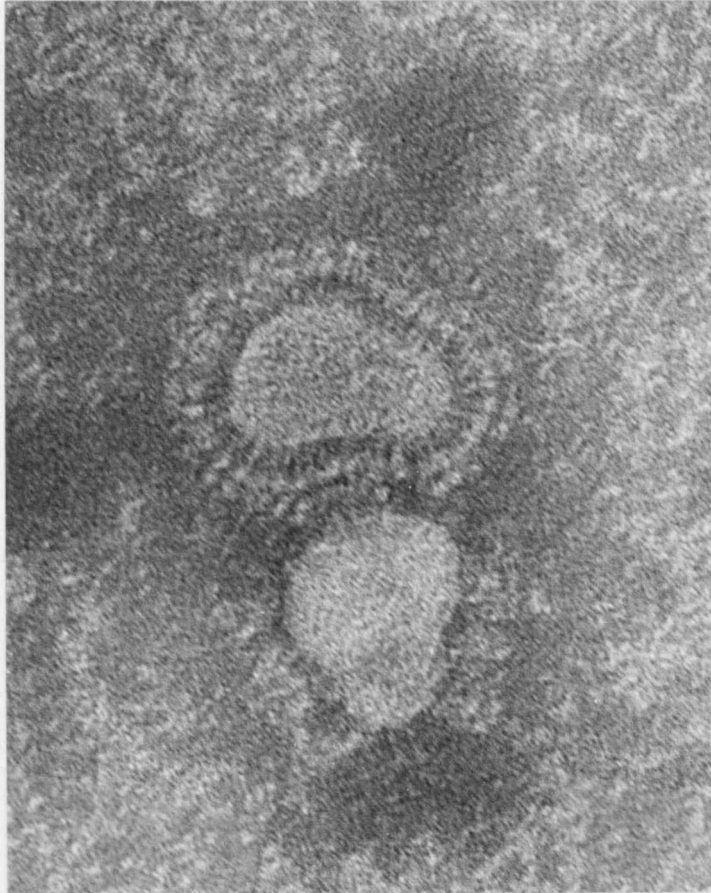


Fig. 3. Negatively stained virion displaying a rosette shape. X390,000.

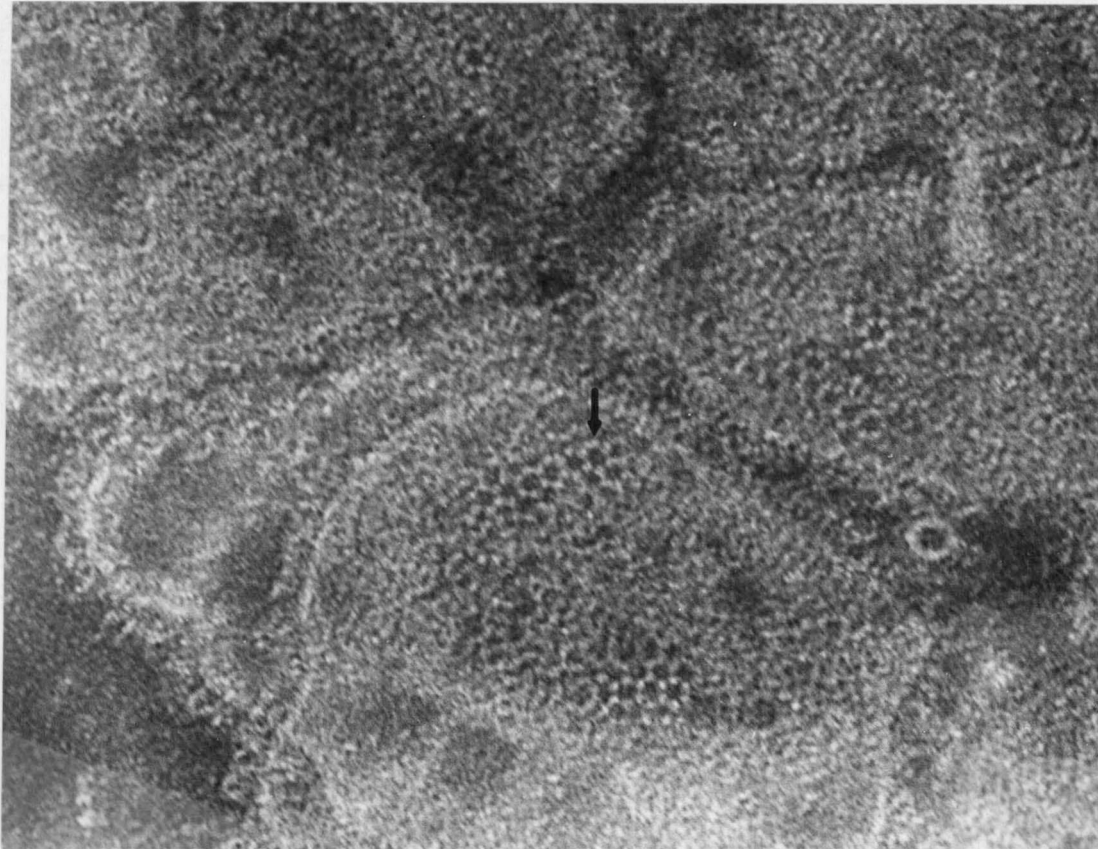


Fig. 4. Negatively stained RS pleomorphic virion. Note the hexagons formed by adjacent surface projections. X300,000.

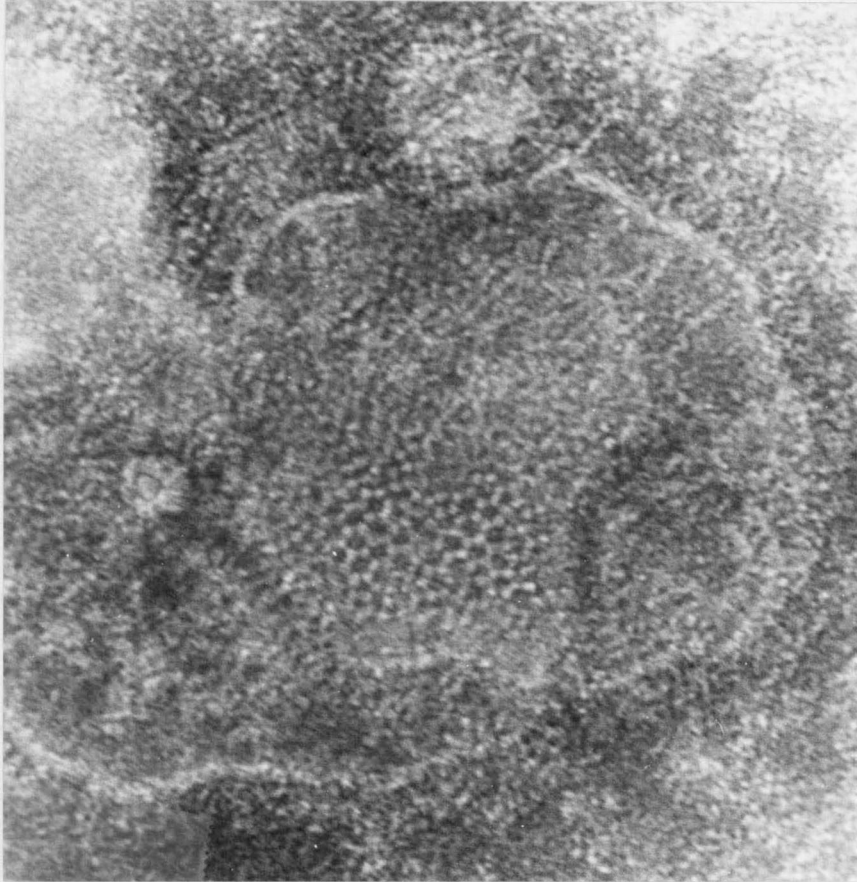


Fig. 5. Negatively stained pleomorphic virion.  
X300,000.

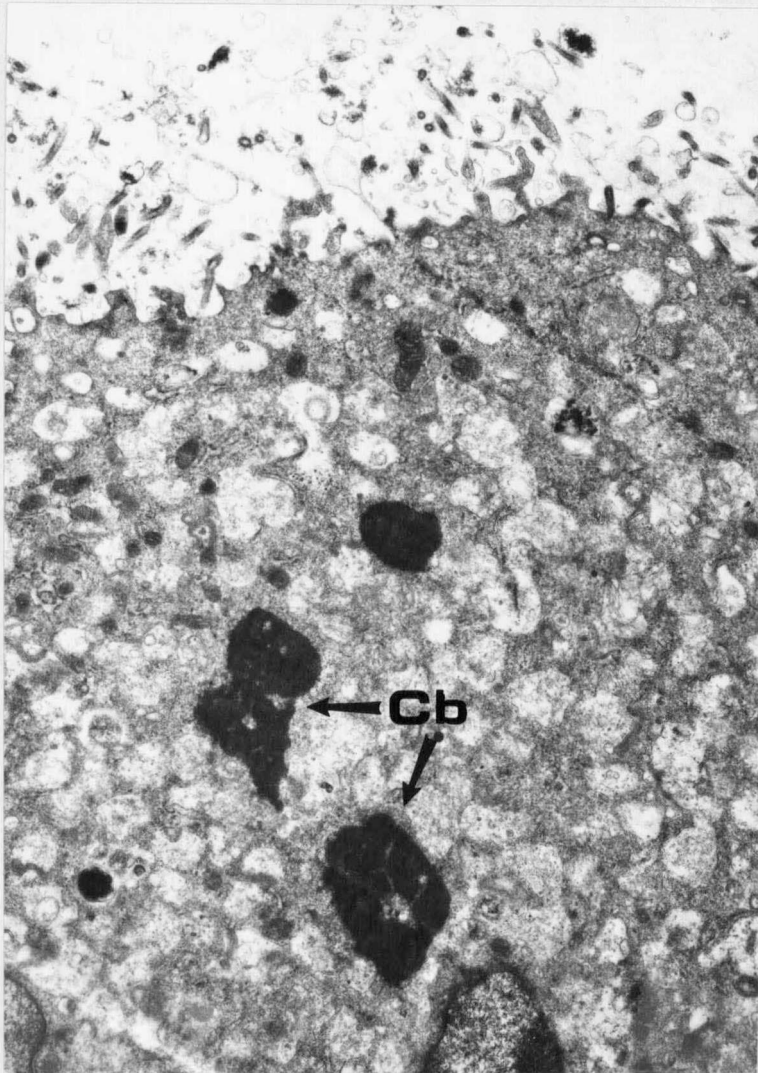


Fig. 6. RSV maturation at the plasma membrane in cell culture. X9,500. Cytoplasmic inclusion bodies (Cb).





Fig. 7. RSV budding from the plasma membrane in cell culture. X45,000. Note electron-dense dots in spherical and filamentous virions. Virions (V).



















































































































































































